Adeno-associated viral transfer of opioid receptor gene to primary sensory neurons: A strategy to increase opioid antinociception

Y. Xu*, Y. Gu*†, G.-Y. Xu*, P. Wu*†, G.-W. Li*, and L.-Y. M. Huang*‡§

*Marine Biomedical Institute, and Departments of †Anatomy and Neurosciences and ‡Physiology and Biophysics, University of Texas Medical Branch, Galveston, TX 77555-1069

Edited by Charles F. Stevens, The Salk Institute for Biological Studies, La Jolla, CA, and approved March 13, 2003 (received for review January 19, 2003)

To develop a genetic approach for the treatment of pain, we introduced a recombinant adeno-associated viral (rAAV) vector containing the cDNA for the μ-opioid receptor (μOR) into primary afferent neurons in dorsal root ganglia (DRGs) of rats, which resulted in a long-lasting (>6 months) increase in μOR expression in DRG neurons. The increase greatly potentiated the antinociceptive effects of morphine in rAAV-μOR-infected rats with and without inflammation. Perforated patch recordings indicated that the efficacy and potency of opioid inhibition of voltage-dependent Ca^{2+} channels were enhanced in infected neurons, which may underlie the increase in opiate efficacy. These data suggest that transfer of opioid receptor genes into DRG cells with rAAV vectors may offer a new therapeutic strategy for pain management.

Chronic pain often causes anguish in patients who suffer from long-term illnesses (e.g., cancer, arthritis, heart disease) or injuries to the nervous system (e.g., spinal cord injury, loss of a limb; ref. 1). Because of their prominent analgesic potency, opiates have remained the drugs of choice for treating many patients with severe pain. The use of opiates, however, sometimes falls short of therapeutic goals because high doses of opiates frequently produce side effects, including respiratory depression, constipation, and tolerance (2–5). New opioid ligands and intrathecal administration have been used to improve opioid efficacy and curtail side effects. More recently, genetic approaches have been attempted (6, 7). Opioid precursor genes, such as those for enkephalin or β-endorphin, were transferred to primary afferent neurons in dorsal root ganglia (DRGs) or the meninges surrounding the spinal cord (7–11). These result in an enhanced production of opioid peptides and a reduction of capsaicin or carrageenan-induced hyperalgesia. However, the antinociceptive effects usually lasted for a short period (1–8 weeks), and some viral vectors produced cytotoxicity. To circumvent these drawbacks, we took a different genetic transfer approach. Recombinant adeno-associated viral (rAAV) vectors, which provide efficient and stable expression in central (12, 13) and peripheral neurons (14, 15), were chosen for gene delivery. A rAAV vector containing the μ-opioid receptor (μOR) gene was introduced into DRGs. Here we show that the μOR expression under the control of a neuron-specific enolase (NSE) promoter results in long-term (>6 months) enhancement of μOR transgene expression in DRG neurons. The enhancement markedly potentiates morphine antinociceptive responses to thermal stimuli under normal and inflamed conditions. The increase in opioid efficacy is in part the result of enhanced blockade of high-threshold voltage-dependent Ca^{2+} channels.

Materials and Methods

All experiments were approved by the Institutional Animal Care and Use Committee at the University of Texas Medical Branch.

Preparation of rAAV Plasmid Constructs and Viral Stocks. The plasmid pTR-NSE and pTR-NSE-enhanced GFP (EGFP) were prepared as described (16). The MOR-1 gene-containing plasmid pCMV-μOR (a gift from H. Akil, Univ. of Michigan, Ann Arbor; ref. 17) was used as the template for PCR amplification to insert a *Sal*I site to the 5′ end and a 6×His peptide sequence followed by a *Hin*dIII site to the 3′ end of the μOR gene. The PCR products were digested by *Sal*I and *Hin*dIII. The resulting fragment was ligated into the *Sal*I/*Hin*dIII sites of pTR-NSE to generate pTR-NSE-μOR. rAAV viral particles were produced in an adenovirus-free system by cotransfecting HEK 293 cells with a rAAV vector plasmid (i.e., pTR-NSE-μOR or pTR-NSE-EGFP), plasmid pXX2, and pXX6 (16, 18). Cells were collected and lysed, and cellular debris was eliminated by centrifugation to gain crude viral solution. The viral solution was fractionated through a Heparin Agarose type I column (Sigma) to yield a purified viral stock.

Infection of DRG Neurons with rAAVs. Primary neuronal cultures were prepared from DRGs of 14-day Sprague–Dawley rats as described (19). Cells were plated onto coverslips and grown in MEM (GIBCO/BRL) with 10% FBS. To infect cultured DRG neurons, a serum-free medium containing 1 μl of viral solution was added to DRG cultures 24–48 h after plating. Ninety minutes later, additional serum (20%)-containing medium was added. The medium was changed within 24 h and every 2–3 days afterward. For *in vivo* experiments, 25- to 30-day-old rats were anesthetized with pentobarbital (50 mg/kg), and left L4 and L5 DRGs were exposed. A viral solution (2 μl) containing either rAAV-μOR or rAAV-EGFP was slowly (15–20 min) injected into each ganglion with a Hamilton syringe. The wound was then closed; animals were returned to their cages.

Morphological Analysis. Cultured DRG cells were fixed with PBS containing 4% paraformaldehyde and 0.2% picric acid at 4°C for 1 h. To obtain tissue sections, injected rats were perfused with the same fixative. DRGs and the spinal cord were then removed and sectioned (10 μm thick) in a cryostat. Morphological integrity of DRGs was examined by staining tissue with hematoxylin/eosin. To detect exogenous μORs, either the monoclonal mouse anti-His antibody (Qiagen, Valencia, CA, 1:20; for cultured DRGs) or the polyclonal rabbit anti-His antibody (Santa Cruz Biotechnology, 1:200; for tissue sections) was used. Fluorescein anti-mouse or anti-rabbit IgG (Vector Laboratories) was the secondary antibody. A polyclonal anti-μOR antibody (DiaSorin, Stillwater, MN, 1:200) was used to label endogenous and exogenous μORs and a rhodamine red-conjugated goat anti-rabbit IgG (Jackson ImmunoResearch) was for visu-

Preliminary results of this work have been published [Xu, Y., Gu, Y., Xu, G.-Y., Wu, P., Li, G.-W. & Huang, L.-Y. M. (2000) *Neurosci. Abstr.* **26,** 1662].

This paper was submitted directly (Track II) to the PNAS office.

Abbreviations: DAMGO, [D-Ala^2,*N*-MePhe^4,Gly^5-ol]enkephalin; EGFP, enhanced GFP; CFA, complete Freund's adjuvant; MPE, maximum possible effect; NSE, neuron-specific enolase; μOR, μ-opioid receptor; rAAV, recombinant adeno-associated viral; DRG, dorsal root ganglion; PWL, paw withdrawal latency.

§To whom correspondence should be addressed. E-mail: lmhuang@utmb.edu.

www.pnas.org/cgi/doi/10.1073/pnas.0930324100

alization. The primary anti-μOR antibody was specific because the antibody pretreated with the μOR peptide immunogen no longer labeled μORs. EGFP was visualized without further treatment. Mouse NeuN (Chemicon, 1:200) was used to label neurons. Mouse anti-N52 (Chemicon, 1:200) was used to label myelinated DRGs; mouse anti-periphrin (Chemicon, 1:200) was used to label cells unmyelinated DRGs. Alexa Fluor 546 goat anti-mouse IgG (Molecular Probes, 1:200) was used for visualization. To avoid the possibility of double-counting, labeled cells in every fifth section were counted.

Western Analyses. Total proteins were extracted from DRGs and the spinal cord of injected rats by using the standard methods (20). Protein extracts (10–30 μg) were subjected to SDS/PAGE (10% acrylamide). Proteins were transferred onto nitrocellulose membranes and subsequently incubated with rabbit anti-μOR antibody (DiaSorin, 1:1,000) for μOR detection. Actin, used as an internal control, was labeled with mouse anti-actin antibody (Chemicon, 1:1,000). Blots were detected by using secondary antisera coupled to horseradish peroxidase and developed by using the enhanced chemiluminescence kit (Amersham Biosciences). Blot intensities were analyzed with a LYNX 5000 image analyzer.

Behavioral Tests. Thermal hyperalgesia to radiant heat was assessed as described (21). Three to four weeks after rAAV injection, rats were acclimated in Plexiglas boxes placed on a platform for 30 min/day for 5 days. To measure paw withdrawal latencies (PWLs), a radiant heat source was placed under the plantar surface of the hind paw and the time elapsed from the onset of radiant heat stimulation to the withdrawal of the paw was recorded. The heat intensity was adjusted to give a baseline latency of ≈10 s; a cutoff time of 30 s was set to prevent possible tissue damage. To obtain baseline PWLs, three measurements separated by a 5-min interval were made for each rat's hind paw and scores were averaged. The antinociceptive effects of morphine were evaluated by measuring PWLs before and every 10 min after the s.c. morphine administration.

To induce inflammation, rats were lightly anesthetized with pentobarbital. Complete Freund's adjuvant (CFA; *Mycobacterium butyricum* from Difco) emulsion (1:1 peanut oil/saline, 1 mg of *Mycobacterium* per ml) was injected into the plantar surface (50 μl) of the rat left hind paw 3–4 weeks after infection of rAAV. Behavioral experiments were performed 5–14 days after the CFA injection.

Perforated Patch Recording. Cells were superfused (2 ml/min) at 23–24°C with external solution containing 130 mM tetraethylammonium (TEA)-Cl, 5 mM CsCl, 1.5 mM $BaCl_2$, 1 mM $MgCl_2$, 10 mM Hepes, and 10 mM glucose (pH 7.2, adjusted with TEA-OH; osmolarity, 300 mosM). Patch electrodes (resistance, 2.2–3.5 MΩ) were filled with internal solution containing 100 mM $CsMeSO_3$, 40 mM CsCl, 10 mM Hepes, and 300 μg/ml amphotericin B (pH = 7.3 adjusted with CsOH, 320 mosM). The currents were filtered at 2–5 kHz and sampled at 100 μs per point. [D-Ala^2,*N*-MePhe^4,Gly^5-ol]enkephalin (DAMGO) was pressure delivered to the recorded cells through a drug applicator (22).

Data Analyses. All data were expressed as mean ± SEM. PWLs obtained from different rats were averaged. Changes before and after morphine treatment within one rat group were analyzed with one-way ANOVA followed by post hoc Newman–Keuls analysis. Antinociceptive responses were expressed as maximum possible effect (MPE) by using the relation MPE = (postdrug PWL − baseline PWL)/(cutoff PWL − baseline PWL) × 100. Dose–response curves were plotted as MPE vs. dose and fitted with the logistic equation. The dose estimated to produce 50% MPE, A50, and 95% confidence intervals were determined. The dose–response curves for DAMGO in current measurements were fitted with the Hill equation, i.e., response = (max − min) × $[IC_{50}/(IC_{50}^n + dose^n)]$ + min, where max and min are maximal and minimal responses, IC_{50} the dose for 50% of the block, and n the Hill coefficient. The 95% confidence band analysis was used to evaluate the significance of the change in the IC_{50} and maximal block. To assess the significance of changes between two means, the Student's t test was used. A $P < 0.05$ was considered significant.

Results

Stable Enhanced Expression of μORs in DRG Neurons Infected with rAAV Vectors. Two rAAV vectors were used in this study. One rAAV vector, used in all of the control experiments, was constructed to express the EGFP gene under the control of a NSE promoter. Another rAAV vector was constructed to contain the rat μOR cDNA in place of the EGFP gene. A 6×His sequence was fused to the C terminus of the μOR gene so that the exogenously introduced μORs could be distinguished from the endogenously expressed μORs with an anti-His antibody. The titer of purified virus, determined by transgene expression in DRG cultures by using a serial dilution of the viral stock, was 4.2×10^8 transducing units (t.u.)/ml for the NSE-EGFP virus (designated as rAAV-EGFP) and 2.6×10^8 t.u./ml for the NSE-μOR virus (rAAV-μOR).

We first investigated μOR expression in cultured DRG neurons treated with rAAV-μOR. The mouse anti-His mAb was used to evaluate the expression of exogenous μORs; the rabbit polyclonal anti-μOR antibody was used to probe the expression of all, i.e., both endogenous and exogenous, μORs. In untreated cultured DRG neurons, none of the neurons were His-positive. About 50.0 ± 2.9% (n = 3) of cells expressed μORs endogenously (data not shown). Five to 7 days after adding crude rAAV-μOR, 60.0 ± 1.7% (n = 6) of DRG neurons were labeled with anti-His antibody (Fig. 1*a Left*) and 81.0 ± 3.6% of cells were labeled with anti-μOR antibody (Fig. 1*a Center*). His-labeled cells were also labeled with anti-μOR antibodies (Fig. 1*a Right*). The μOR fluorescence in doubled-labeled neurons was usually much brighter than that in single-labeled neurons. Their cell processes were often labeled intensely. When purified rAAV-μOR was used, >90% of cultured DRG neurons became His-positive (Fig. 1*b*).

To infect DRG neurons with rAAV-μOR *in vivo*, a purified viral stock of rAAV-μOR was injected into the L4 and L5 ganglia (2 μl each). The rats showed no signs of paresis or other abnormalities afterward. The injected DRGs, stained with hematoxylin/eosin, retained their structural integrity; leukocytes were not present in the ganglia. The immune responses due to rAAV-μOR infection were therefore minimal. Studies of three animals in each rat group, 37.3% of neurons in the injected DRGs were brightly labeled with rabbit polyclonal anti-His antibody 3 weeks after the injection. (Fig. 1*c Left*). A majority (≈25%) of them were small [diameter (d) < 25 μm] and medium ($25 < d < 35$ μm) neurons, which likely mediate nociception. All His-positive neurons were also NeuN-positive (Fig. 1*c Center* and *Right*), confirming the neuron specificity of the NSE promoter. The expression remained stable for at least 6 months. No His-labeled cells were found in the DRGs contralateral to the injected side. In injected DRGs, anti-μOR antibody labels were found in 76.3% of cells, a percentage significantly higher than the 50.1% of labeled neurons on the contralateral side (Figs. 1 *d* and *e*). The increase in percentages of neurons expressing μORs suggests that the rAAV-μOR viron indeed infects neurons, many of which do not express or minimally express μORs endogenously. We also examined His labels in the spinal cord. His label was seen in axons and presumed nerve terminals in the dorsal column and laminae I–V of the spinal cord ipsi-, but not

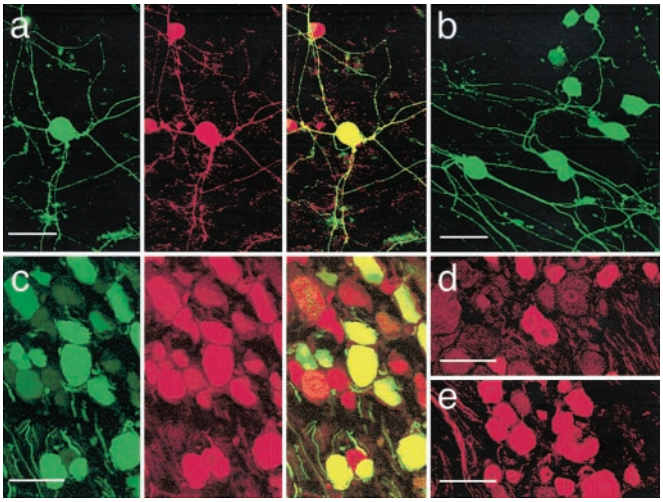

Fig. 1. Expression of μOR *in vitro* and *in vivo*. (*a*) His-peptide (*Left*) and μOR (*Center*) labels in cultured DRG neurons. Cells were examined under a confocal microscope 2 weeks after they were infected with crude rAAV-μOR. The soma and processes of the neuron in the center were intensely labeled with both antibodies. In the merged image (*Right*), the yellow fluorescent cell contained exogenous μORs. Red fluorescent cells contained only endogenous μORs. (*b*) His-labeled cultured DRG neurons 2 weeks after infection with purified rAAV-μOR. Most cells (>90%) were His-positive. (*c*) His (*Left*) and NeuN (*Center*) labels in *in vivo* DRGs 3 weeks after the injection of rAAV-μOR. The merged image (*Right*) shows that His labels are present only in NeuN-positive cells, suggesting neuronal specificity of the NSE promoter. (*d*) Anti-μOR antibody labels in a ganglion contralateral to the injection side 3 weeks after rAAV-μOR injection. Studies of three animals indicated that ≈50.1% of neurons expressed μORs endogenously. (*e*) In the ganglion ipsilateral to the injection, considerably more (76.3%) and brighter μOR-labeled cells were observed. (Bars = 50 μm.)

contralateral, to the injection; no spinal neuron cell bodies were labeled (data not shown).

We further investigated the type of DRG neurons, i.e., nociceptive and nonnociceptive neurons, infected by rAAV. With some exceptions, it is generally believed that large ($d > 35$ μm) and myelinated neurons mediate nonnociceptive sensations and small ($d < 25$ μm) and medium ($25 < d < 35$ μm) unmyelinated or myelinated neurons mediate nociception (23). Neuronal types were therefore categorized according to their sizes and myelination. Almost all DRG neurons in the culture were His-labeled (Fig. 1*b*), suggesting that rAAV infected both nociceptive and nonnociceptive neurons. However, μOR expression in nonnociceptive neurons *in vitro* was difficult to assess quantitatively because large DRG neurons did not survive as well as small and medium neurons in cultures. The μOR expression was therefore quantified *in vivo*. Because mouse monoclonal His-antibody could not optimally label μORs *in vivo*, rabbit polyclonal His-antibody had to be used, which prevented us from double-labeling μORs *in vivo* with anti-His and anti-μOR antibodies. Different strategies were used. We first determined the percentages of neurons labeled with the anti-μOR antibody in the DRGs ipsi- and contralateral to the rAAV injection (Table 1). We found that higher percentage of neurons expressing μORs in ipsilateral DRGs. The increase in percentages of neurons expressing μORs (i.e., small cell, 6.8%; medium cells, 9.4%; large cell, 10.0%) suggests that the rAAV-μOR viron indeed infects neurons, many of which do not express μORs endogenously. We next double-labeled DRGs with rabbit anti-His antibody and mouse anti-N52, which labels myelinated DRGs (24), or mouse antiperipherin, which labeled unmyelinated DRGs (25). About 7.3% of small cells, 17.8% of medium cells, and 12.2% of large cells were His-labeled (Table 1). These

Table 1. DRG neuronal types infected by rAAV-μOR

	Small cell, $d < 25$ μm*	Medium cell, $25 < d < 35$ μm	Large cell, $d > 35$ μm	Total†
μOR-labeled‡				
Contralateral	26.2 ± 2.8	19.8 ± 1.7	4.1 ± 0.3	50.1
Ipsilateral	33.0 ± 2.5	29.2 ± 2.2	14.1 ± 0.4	76.3
Increase§	6.8	9.4	10.0	26.2
Double-labeled¶				
His + N52	2.2 ± 0.02	9.8 ± 0.08	12.2 ± 0.3	24.2
His + peripherin	5.1 ± 0.03	8.0 ± 0.1	0	13.1
Sum‖	7.3	17.8	12.2	37.3

Total number of cells counted was set as 100%. All values stated are in percent.
*d = cell diameter.
†Total = total percentage of labeled cells, including small-, medium-, and large-sized cells.
‡Cells labeled with anti-μOR antibody.
§Increase = (ipsilateral − contralateral).
¶Cells double-labeled with anti-His and anti-His or anti-His and antiperipherin antibodies.
‖Sum = sum of the percentages of double-labeled cells.

percentages were larger than the percentage increases examined with the anti-μOR antibody. These results suggest that rAAVs also infect neurons, especially medium-sized, that express μORs endogenously. Furthermore, two-thirds [i.e., (7.3 + 17.8)/37.3 = 0.67] of exogenous μORs were expressed in small and medium neurons, which likely mediate nociception. A third of exogenous μORs were expressed in large, presumably nonnociceptive, cells.

The rAAV-derived increase in μOR expression was further quantified by Western blot analyses. The injected and contralateral ganglia were removed from the animals at different time points and probed with the anti-μOR antibody. Compared with the contralateral ganglia, μOR expression in the injected DRGs increased with time, plateaued at ≈2-fold 14 days after the injection (Fig. 2*a*). The delay in reaching the plateau is likely caused by the time for the AAV, which is a single-stranded replication-defective DNA virus, to convert from single- to doubled-stranded DNA (26). Once it reached a plateau, μOR expression remained stable up to 6 months (the longest time point tested; Fig. 2*a*). The μOR expression in the spinal-cord segments innervated by the L4 and L5 ganglia was increased with a similar time course and reached a maximum increase of 1.5-fold (Fig. 2*b*). We also compared μOR expression in the DRG and spinal cord before and after inflammation by using Western analyses (Fig. 2*c*). The relative blot intensity, i.e., μOR expression, in the DRG and spinal cord of normal saline and rAAV-EGFP rats after inflammation were not significantly different from their contralateral controls. The μOR expression of rAAV-μOR rats was considerably higher than the contralateral control (DRG: non-CFA = 1.96 ± 0.02, CFA = 1.94 ± 0.07; spinal cord: non-CFA = 1.48 ± 0.10, CFA = 1.49 ± 0.07). However, inflammation did not significantly alter μOR expression.

Enhanced Antinociceptive Effects of Morphine in rAAV-μOR Rats. To determine the functional consequence of the enhanced expression of μORs, we studied the effects of morphine on thermal nociceptive responses, which are mediated by small and medium DRG neurons, in rAAV-injected rats. The left L4–L5 ganglia of rats were injected with either the rAAV-EGFP or rAAV-μOR. Three to four weeks later, PWLs to noxious radiant heat were measured from the hind paw ipsilateral to the rAAV injection. The basal PWLs for rats infected with rAAV-μOR and rAAV-EGFP were indistinguishable (PWL = 10.08 ± 0.45 s, $n = 34$ for rAAV-EGFP rats; PWL = 10.29 ± 0.46 s, $n = 36$ for rAAV-

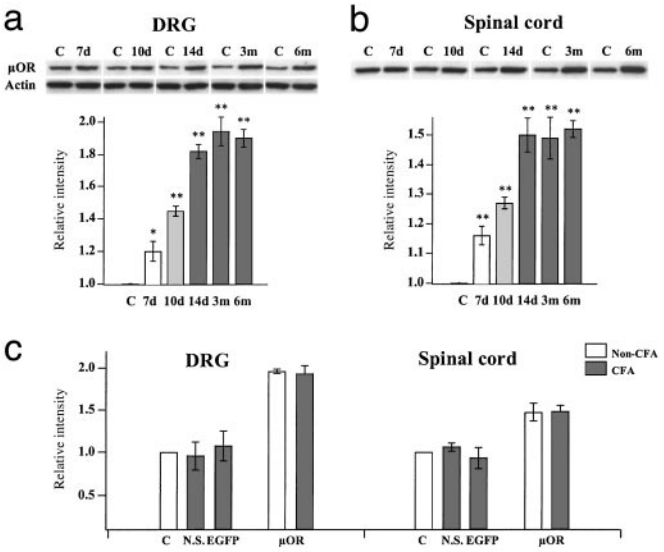

Fig. 2. Western analyses of μOR expression. L4 and L5 DRGs (*a*) and the dorsal spinal cord (*b*) ipsilateral to the rAAV injection were removed from animals at various times and the expression of μORs was probed with the anti-μOR antibody. The intensities of protein bands (≈51 kDa) were normalized with actin in the sample. The μOR expression on the contralateral side (C) was set at 1.0. The μOR expression in DRG cells increased with time and approached a plateau of ≈2-fold 14 days after infection. The μOR expression in the spinal cord reached a maximum of 1.5-fold. The expression in both DRGs and the spinal cord remained stable for at least 6 months (*, $P < 0.05$; **, $P < 0.01$). (*c*) μOR expression after inflammation. CFA was injected in the left paw of rats 3–4 weeks after rAAV infection. Ten days after CFA injection, DRGs and the spinal cord were removed. The μOR expression in inflamed rats injected with normal saline (N.S.) or rAAV-EGFP (EGFP) was not significantly different from the contralateral controls. The μOR expression in the ipsilateral DRGs or spinal cord of rAAV-μOR rats was significantly higher than the contralateral controls. Inflammation did not change the μOR expression.

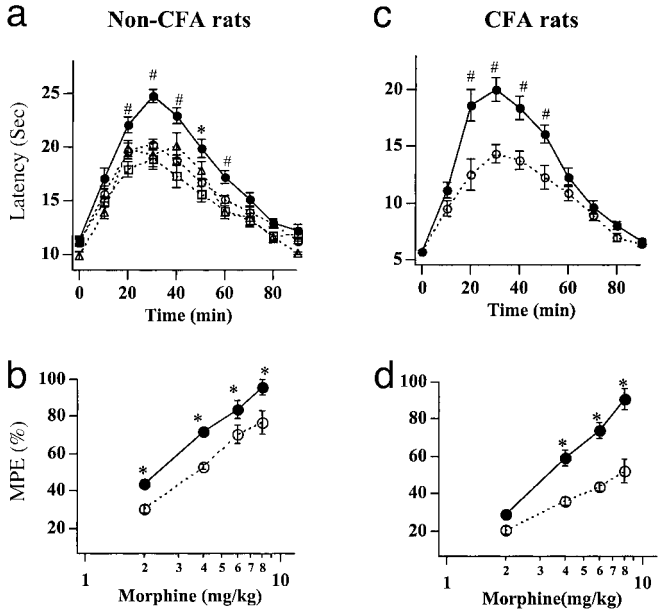

Fig. 3. Morphine antinociceptive effects are enhanced in rAAV-μOR-injected rats. (*a*) The PWLs after the treatment of 4 mg/kg morphine in non-CFA (uninflamed) rats. The antinociceptive effects reached a maximum by 30–40 min and then gradually dissipated in 80–90 min. The PWLs obtained from the rat paw ipsilateral to the rAAV-EGFP (○; $n = 12$) or normal saline (△; $n = 6$) injection or from the paw contralateral to the rAAV-μOR injection (□; $n = 6$) were all similar. In contrast, the PWLs obtained from the paw ipsilateral to the rAAV-μOR injection (●; $n = 10$) were larger, suggesting an enhanced antinociceptive effect of morphine. (*b*) Morphine dose–response curves for non-CFA rats injected with rAAV-EGFP or rAAV-μOR. For all morphine doses, the antinociceptive responses of morphine, expressed in MPEs, in rAAV-μOR rats were significantly enhanced ($n = 5$). (*c* and *d*) In CFA (inflamed) rats, the antinociceptive effect of morphine in rAAV-μOR rats was even more enhanced. The PWLs obtained from rAAV-μOR rats (●; $n = 5$) were much larger than those from rAAV-EGFP rats (○; $n = 5$; *, $P < 0.05$; #, $P < 0.01$).

μOR rats). In both rat groups, a s.c. morphine injection produced an increase in the PWL, and the antinociceptive effect developed with a similar time course (Fig. 3*a*). However, the PWLs in rAAV-μOR rats were larger than those measured in rAAV-EGFP rats. To make sure that rAAV-EGFP itself did not produce unforeseeable behavioral consequences, we examined morphine antinociceptive effects on the paw contralateral to the rAAV-μOR injection ($n = 6$) and the paw in rats with saline injected in their DRGs ($n = 7$). The behavioral responses in these two control groups were similar to the rats treated with rAAV-EGFP (Fig. 3*a*). Most control experiments hereafter were done with rAAV-EGFP rats. The enhanced effect of morphine in rAAV-μOR rats was observed consistently at different morphine doses. Therefore, the morphine dose–response, expressed as the MPE, for rAAV-μOR rats was shifted to the left of that for rAAV-EGFP rats (Fig. 3*b*). The morphine dose to produce 50% MPE, i.e., A50, was 2.34 mg (95% confidence limits, 1.78–2.88 mg) for rAAV-μOR rats and was 3.63 mg (2.95–4.27 mg) for rAAV-EGFP. The increased antinociceptive effects of morphine persisted in rAAV-μOR rats for at least 3 months (the longest period tested).

We also studied the morphine effects on thermal nociceptive responses in rAAV-EGFP and rAAV-μOR rats with inflammation. CFA was injected into the hind paw and nociceptive responses were examined 5–14 days later. Compared with non-CFA-treated rats, the basal PWLs to heat were considerably reduced (PWL = 6.02 ± 0.35 s, $n = 12$ for rAAV-EGFP rats; PWL = 5.92 ± 0.33 s, $n = 19$ for rAAV-μOR rats). Morphine treatment increased the PWLs in both rAAV-EGFP and rAAV-μOR rat groups (Fig. 3*c*). The nociceptive effects of morphine in rAAV-μOR rats were again larger than those in rAAV-EGFP rats. The extent of increase in PWLs induced by rAAV-μOR treatment was more pronounced in CFA rats (Fig. 3*c*) than in non-CFA rats (Fig. 3*a*). This finding could also be seen in morphine dose–response curves (Fig. 3*d*). The increase in the MPEs of rAAV-μOR rats, especially for morphine doses ≥4 mg/kg, was larger after CFA treatment. The A50 for rAAV-μOR rats was 2.63-fold lower than that for rAAV-EGFP rats [rAAV-μOR, A50 = 3.02 mg (2.75–3.31 mg); rAAV-EGFP, A50 = 7.94 mg (6.6–9.3 mg)]. Thus, enhanced μOR expression increases the efficacy of morphine; the increase is further potentiated after inflammation. Comparing the morphine dose–response curves of non-CFA and CFA-treated rAAV-EGFP rats, the dose–response curve of CFA-treated rAAV-EGFP rats was shifted to the right (non-CFA, A50 = 3.64 mg; CFA, A50 = 7.94 mg) (Fig. 3 *b* and *d*). That is, more opiates are required to overcome the enhanced nociception caused by inflammation. In contrast, the shift in morphine dose–response curve in rAAV-μOR rats before and after inflammation (non-CFA, 2.34 mg; CFA, A50 = 3.02 mg) was not statistically significant, a result of the much more pronounced enhancement of antinociceptive effect of morphine in rAAV-μOR rats after inflammation.

Enhanced Block of Ca^{2+} Channels in rAAV-μOR-Infected Neurons. It is well established that μ-opioids inhibit high-threshold voltage-dependent Ca^{2+} currents in DRG neurons (27, 28). To determine whether the enhanced μOR expression alters opioid inhibition of Ca^{2+} currents, we compared the effects of the

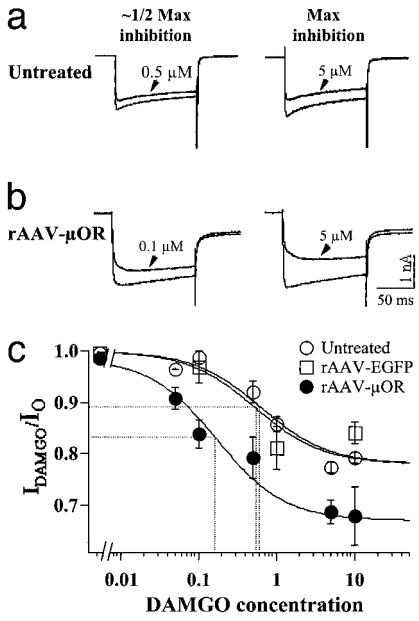

Fig. 4. DAMGO exerts stronger inhibitory effects on Ca^{2+} channels in isolated DRG neurons infected with rAAV-μOR. Ba^{2+} currents recorded before and after DAMGO treatment in untreated (*a*) and rAAV-μOR-infected (*b*) DRG cells. The DAMGO doses for about half-maximal and maximal inhibition are indicated. DAMGO induced larger maximal inhibition and produced about half-maximal inhibition at a lower dose in rAAV-μOR cells. Membrane potentials were held at -60 mV. (*c*) Dose dependence of Ca^{2+} channel inhibition by DAMGO after rAAV-μOR infection. The Ca^{2+} channel currents were measured at different concentrations of DAMGO. Cells insensitive to DAMGO were not included in the analysis. Data were fit with the Hill equation with Hill coefficient = 1. The maximal inhibition for rAAV-μOR cells was 31.63%, which was significantly larger than that for untreated and rAAV-EGPF cells ($\approx$22%). The IC_{50} for rAAV-μOR cells was 3- to 4-fold smaller than for control cells. The data were obtained from 3 to 24 cells.

μ-opioid agonist, DAMGO, on the activity of high-threshold Ca^{2+} channels in untreated, rAAV-EGFP-treated, and rAAV-μOR-treated cultured DRG neurons. rAAV virons were added to neurons 1–2 days after plating. Seven days after the infection, perforated patch whole-cell recordings were performed on the cells. External Ca^{2+} was replaced by Ba^{2+} to avoid rapid rundown of current responses. DAMGO was found to block Ba^{2+} currents in small and medium DRG cells (diameter, 18–35 μm). The block was observed for both control (untreated and rAAV-EGFP-treated) and rAAV-μOR-treated DRG neurons (Fig. 4). However, a larger percentage of cells responded to DAMGO inhibition in the rAAV-μOR group (89.2%, $n = 34$) than that in the control groups (untreated cells, 57.1%, $n = 14$; rAAV-EGFP, 54.5%, $n = 11$). In addition, the maximal block of Ba^{2+} currents in rAAV-μOR cells was significantly higher (Fig. 4 *a* and *b*). The slowing of activation of the currents in rAAV-μOR neurons became more evident. The DAMGO dose required for about half-maximal inhibition in rAAV-μOR cells was severalfold lower than that in the control groups (Fig. 4*c*). When the dose–response curves of the DAMGO block was fit with the Hill equation, the maximal block was about 22.02 $\pm$ 0.01% for untreated cells, 22.02 $\pm$ 0.01% for rAAV-EGFP cells, and 31.63 $\pm$ 0.03% for rAAV-μOR cells. The apparent affinity for DAMGO inhibition (IC_{50}) was 0.53 $\pm$ 0.03 μM for the rAAV-EGFP and 0.64 $\pm$ 0.19 for the untreated cells. The IC_{50} was 0.17 $\pm$ 0.06 μM for the rAAV-μOR cells, a 3.1- or 3.8-fold increase in the affinity. Therefore, the potency and efficacy of opioid inhibition are significantly increased after rAAV-μOR infection.

Discussion

Introducing transgenes into nociceptive-related neurons presents an exciting therapeutic alternative for the treatment of pain. The technique allows a specific protein to be synthesized and exert its effects in the targeted tissue, thus reducing or even eliminating the problems of short half-life and side effects of classical drugs. Poor gene transfer efficacy, transient transgene expression and toxicity, or immune responses, however, have limited the success of such a genetic approach. Here, we show that these obstacles can be largely circumvented by using rAAV vectors. rAAV under the control of the NSE promoter efficiently drives the expression of μORs exclusively in DRG neurons (Fig. 1). Toxic effects or immune responses of rAAV infection were not evident. The expression of μORs remained stable during the period when DRG cultures were viable (3–4 weeks). Furthermore, we demonstrate here an abundant and stable expression of μORs in DRGs and their terminals after rAAV-μOR infection. Most exogenous μORs are expressed in small and medium, presumably, nociceptive neurons. We also found that rAAV-μOR infects both neurons with minimal endogenous μORs and neurons that express μORs endogenously (Table 1). Therefore, the enhanced antinociceptive effects of morphine observed in rAAV-μOR rats (Fig. 3) could be attributed to more nociceptive neurons that are sensitive to opioids and to enhanced sensitivity to opioids in those neurons that have μORs endogenously. The latter is consistent with the finding that a large number of nociceptors express μOR at levels well below its maximal opioid sensitivity (29). Our observation that exogenous μOR expression is limited to DRGs and their terminals agrees with others that gene products caused by rAAV seldom appear at transsynaptic locations (12). By targeting presynaptic DRG neurons instead of postsynaptic cells, which include both excitatory and inhibitory neurons in the superficial spinal cord, for infection, some unexpected consequences of descending facilitation are avoided (30). We also found that a substantial number of μORs are expressed in myelinated large DRG cells that do not express endogenous μORs (Table 1) and are presumably nonnociceptive. The behavioral consequences of this change are of great interest and under investigation.

Our behavioral studies show that the increase in μORs does not affect basal nociceptive responses under normal or inflamed conditions, but it significantly enhances the antinociceptive effects of morphine (Fig. 3). The increased morphine antinociceptive action correlates well with the increased μOR expression for at least 3 months (the longest period tested) after infection. Although the mechanisms underlying the increased morphine antinociceptive effect remain to be thoroughly delineated, our studies indicate that the increased antinociceptive responses could arise from the enhanced efficacy and potency of μ-opioid to inhibit voltage-dependent Ca^{2+} currents (Fig. 4). It is well established that a block of Ca^{2+} channels at the central presynaptic terminals of DRG cells profoundly affects synaptic transmission in the spinal cord (31–33). An increase in opioid block of Ca^{2+} channels in rAAV-μOR neurons could give rise to the enhanced opioid inhibition of nociceptive signals in the sensory neurons.

We found that in the control rat groups more opiates are required to overcome the enhanced nociception in the inflammatory state (Fig. 3 *b* and *d*). This result is consistent with the study of Gutstein *et al.* (34) but is different from other studies that show an enhancement of the antinociceptive effect of morphine after inflammation (35). The discrepancies among various studies could be attributed to dissimilar inflammatory conditions, different rat species, and varying stress levels induced in animals during behavioral experiments (36). Some suggest that the enhancing effect of opioids results from inflammation-induced spontaneous up-regulation of μORs in the DRG (37).

However, our Western analyses show that inflammation does not change μOR expression in the DRG (Fig. 2), a result consistent with the finding that mRNA levels in the DRG remain unchanged after inflammation (38). Schafer *et al.* (38) showed that peripherally applied μ-opioids produce enhanced analgesic effects in the inflamed paw. They suggested that the enhancement may be produced by an increased axonal transport of μORs in the sciatic nerve and thus an increase in opioid receptors in peripheral nerve terminals (39). It is of interest to determine whether the level of peripheral opioid receptors in rAAV-μOR rats changes in the inflammatory state. One interesting observation is that rAAV-μOR infection causes a more pronounced increase in morphine efficacies in the inflammatory state (Fig. 3). As a result, inflammation no longer induces rightward shift in the morphine dose–response curve. This potentiation of morphine effects in CFA treated rAAV-μOR rats clearly is of potential therapeutic interest; the mechanism for the increase needs to be determined. Preferential up-regulation of endogenous opioid peptides after inflammation (35, 40) could be one factor contributing to the increase in morphine efficacy in inflamed rAAV-μOR rats.

Our strategy of up-regulating opioid receptor expression in DRGs is different from those of others to deliver opioid genes in the nociceptive system (7–9). Because the release of opioids depends on neuronal activity, which is enhanced during nociception, an increase in opioid production would potentiate opioid release, thus reducing basal nociceptive responses after inflammation. On the other hand, chronic nociceptive conditions may induce excessive and prolonged release of opioids thus promoting the development of tolerance. Our approach to up-regulate μORs does not depend on afferent activity. Therefore, basal nociceptive responses are unaffected under either normal or inflamed conditions. The possibility of using low doses of opioids for antinociception at a reduced risk of tolerance development after the rAAV-μOR infection (Figs. 3 and 4) strongly suggests the therapeutic potential of this approach.

The key advantages of our strategy to up-regulate opioid receptors are: (*i*) the rAAV viral system induces an efficient and long-lasting (up to 6 months) receptor expression; (*ii*) the transgene expression can target specifically to DRG neurons, thus avoiding undesired systemic effects of opioids; (*iii*) the increased μOR expression results in a significant enhancement in the antinociceptive effects of morphine; and (*iv*) the increase in morphine efficacy is further enhanced in the inflammatory state. Furthermore, the stable and specific targeted expression of opioid receptors in rats provides a good model system for determining behavioral consequences and mechanisms underlying this gene transfer approach. A possible disadvantage is that direct injection of rAAV into the DRG could incur tissue damage and thus limits its application in gene therapy. With further refinement in vector design, receptor manipulation, and routes of gene delivery, rAAV opioid receptor infection can be a valid therapeutic strategy for the treatment of acute and chronic pain in humans. Moreover, the same approach can be adapted for other molecules associated with pain processing to provide new ways to alleviate pain resulting from injuries or diseases.

We thank Drs. W. Willis and R. E. Coggeshall for comments. This research was supported by National Institutes of Health Grants NS30045, NS11255, and DA13668.

1. Woolf, C. J. & Salter, M. W. (2000) *Science* **288,** 1765–1769.
2. Fairbanks, C. A. & Wilcox, G. L. (1997) *J. Pharmacol. Exp. Ther.* **282,** 1408–1417.
3. Vanderah, T. W., Gardell, L. R., Burgess, S. E., Ibrahim, M., Dogrul, A., Zhong, C. M., Zhang, E. T., Malan, T. P., Jr., Ossipov, M. H., Lai, J. & Porreca, F. (2000) *J. Neurosci.* **20,** 7074–7079.
4. Williams, J. T., Christie, M. J. & Manzoni, O. (2001) *Physiol. Rev.* **81,** 299–343.
5. Yaksh, T. L. (2000) *Pain Res. Manage.* **5,** 19–22.
6. Wilson, S. P. & Yeomans, D. C. (2000) *Curr. Rev. Pain* **4,** 445–450.
7. Pohl, M. & Braz, J. (2001) *Eur. J. Pharmacol.* **429,** 39–48.
8. Finegold, A. A., Mannes, A. J. & Iadarola, M. J. (1999) *Hum. Gene Ther.* **10,** 1251–1257.
9. Wilson, S. P., Yeomans, D. C., Bender, M. A., Lu, Y., Goins, W. F. & Glorioso, J. C. (1999) *Proc. Natl. Acad. Sci. USA* **96,** 3211–3216.
10. Beutler, A. S., Banck, M. S., Bach, F. W., Gage, F. H., Porreca, F., Bilsky, E. J. & Yaksh, T. L. (1995) *J. Neurochem.* **64,** 475–481.
11. Braz, J., Beaufour, C., Coutaux, A., Epstein, A. L., Cesselin, F., Hamon, M. & Pohl, M. (2001) *J. Neurosci.* **21,** 7881–7888.
12. Chamberlin, N. L., Du, B., de Lacalle, S. & Saper, C. B. (1998) *Brain Res.* **793,** 169–175.
13. Peel, A. L., Zolotukhin, S., Schrimsher, G. W., Muzyczka, N. & Reier, P. J. (1997) *Gene Ther.* **4,** 16–24.
14. Glatzel, M., Flechsig, E., Navarro, B., Klein, M. A., Paterna, J. C., Bueler, H. & Aguzzi, A. (2000) *Proc. Natl. Acad. Sci. USA* **97,** 442–447.
15. Fleming, J., Ginn, S. L., Weinberger, R. P., Trahair, T. N., Smythe, J. A. & Alexander, I. E. (2001) *Hum. Gene Ther.* **12,** 77–86.
16. Wu, P., Ye, Y. & Svendsen, C. N. (2002) *Gene Ther.* **9,** 245–255.
17. Thompson, R. C., Mansour, A., Akil, H. & Watson, S. J. (1993) *Neuron* **11,** 903–913.
18. Xiao, X., Li, J. & Samulski, R. J. (1998) *J. Virol.* **72,** 2224–2232.
19. Huang, L. Y. & Neher, E. (1996) *Neuron* **17,** 135–145.
20. Sambrook, J., Fritsch, E. F. & Maniatis, T. (1989) in *Detection and Analysis of Proteins Expressed from Cloned Genes*, ed. Nolan, C. (Cold Spring Harbor Lab. Press, Plainview, NY), Vol. 3, pp. 18.60–18.75.
21. Hargreaves, K., Dubner, R., Brown, F., Flores, C. & Joris, J. (1988) *Pain* **32,** 77–88.
22. Xu, G. Y. & Huang, L. Y. (2002) *J. Neurosci.* **22,** 93–102.
23. Willis, W. D. & Coggeshall, R. (1991) *Dorsal Root Ganglion Cells and Their Processes* (Plenum, New York), pp. 47–78.
24. Shaw, G., Osborn, M. & Weber, K. (1986) *Eur. J. Cell Biol.* **42,** 1–9.
25. Garcia-Anoveros, J., Samad, T. A., Zuvela-Jelaska, L., Woolf, C. J. & Corey, D. P. (2001) *J. Neurosci.* **21,** 2678–2686.
26. Ferrari, F. K., Samulski, T., Shenk, T. & Samulski, R. J. (1996) *J. Virol.* **70,** 3227–3234.
27. Schroeder, J. E. & McCleskey, E. W. (1993) *J. Neurosci.* **13,** 867–873.
28. Moises, H. C., Rusin, K. I. & Macdonald, R. L. (1994) *J. Neurosci.* **14,** 3842–3851.
29. Silbert, S. C., Beacham, D. W. & McCleskey, E. W. (2003) *J. Neurosci.* **23,** 34–42.
30. Vanderah, T. W., Ossipov, M. H., Lai, J., Malan, T. P., Jr., & Porreca, F. (2001) *Pain* **92,** 5–9.
31. Kohno, T., Kumamoto, E., Higashi, H., Shimoji, K. & Yoshimura, M. (1999) *J. Physiol. (London)* **518,** 803–813.
32. Iwasaki, S., Momiyama, A., Uchitel, O. D. & Takahashi, T. (2000) *J. Neurosci.* **20,** 59–65.
33. Gruner, W. & Silva, L. R. (1994) *J. Neurosci.* **14,** 2800–2808.
34. Gutstein, H. B., Trujillo, K. A. & Akil, H. (1995) *Brain Res.* **680,** 173–179.
35. Stanfa, L. & Dickenson, A. (1995) *Inflamm. Res.* **44,** 231–241.
36. Gutstein, H. B. (1996) *Pharmacol. Rev.* **48,** 403–411.
37. Zhang, Q., Schaffer, M., Elde, R. & Stein, C. (1998) *Neuroscience* **85,** 281–291.
38. Schafer, M., Imai, Y., Uhl, G. R. & Stein, C. (1995) *Eur. J. Pharmacol.* **279,** 165–169.
39. Hassan, A. H., Ableitner, A., Stein, C. & Herz, A. (1993) *Neuroscience* **55,** 185–195.
40. Spetea, M., Rydelius, G., Nylander, I., Ahmed, M., Bileviciute-Ljungar, I., Lundeberg, T., Svensson, S. & Kreicbergs, A. (2002) *Eur. J. Pharmacol.* **435,** 245–252.